THE JOURNAL OF PHYSICAL CHEMISTRY A

Article

Cite This: J. Phys. Chem. A 2019, 123, 8385−8390

pubs.acs.org/JPCA

Sulfuric Acid Formation via H_2SO_3 Oxidation by H_2O_2 in the Atmosphere

Svetlana Shostak,[†] Kitae Kim,[‡,§] Yevhen Horbatenko,*[,†] and Cheol Ho Choi*[,†]

[†]Chemistry Department, Kyungpook National University, Daehak-ro 80, Daegu 41566, Republic of Korea

[‡]Korea Polar Research Institute (KOPRI), Incheon 21990, South Korea

[§]Department of Polar Sciences, University of Science and Technology (UST), Incheon 21990, South Korea

Supporting Information

ABSTRACT: With the help of quantum mechanical methods, the formation of H_2SO_4 by the oxidation of H_2SO_3 with H_2O_2 was studied theoretically. Both stepwise and concerted mechanisms were calculated. It was found that the direct oxidation of H_2SO_3 by H_2O_2 alone requires prohibitive activation energies of >38.6 kcal/mol. However, the addition of one water molecule exhibits a strong catalytic effect that dramatically reduces the overall reaction barrier to 6.2 (2.3 with PCM) kcal/mol. The deprotonated HSO_3^- species also reduces the overall reaction barrier to 5.6 (−5.8 with PCM) kcal/mol. Both of these proceed via concerted pathways. On the other hand, the stepwise mechanisms generally produce intermediates with a hydroperoxy group (−O−O−H), which is a result of a nucleophilic attack by the oxygens of H_2O_2. While studying the catalytic effect of water, a previously unknown hydroperoxy intermediate $(HOO)S(OH)_3$, where sulfur is coordinated with three OH groups, was found. This work also reveals a rearrangement step of another hydroperoxy intermediate $(HOO)SO_2^-$ to HSO_4^- that was found in earlier experimental studies. For all of the mechanisms calculated, the final H_2SO_4 is formed with a significant exothermicity of >60 kcal/mol. In general, even without sunlight, it was found that the formation of sulfuric acid by hydrogen peroxide can occur in a heterogeneous moisturized environment.

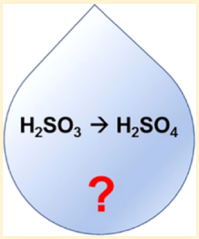

1. INTRODUCTION

Sulfur-containing compounds play a major role in the atmospheric aerosols formation.[1] A high concentration of long-lived sulfur species is detected in the atmosphere around industrial regions due to anthropogenic SO_2 emission. The lifetime of sulfate aerosols in the troposphere is found to be several days.[2] These species have a significant impact on Earth's climate,[2] environment, and human health.[3] For example, acid rains due to the presence of H_2SO_4 in the atmosphere are a critical problem especially for regions with a high level of air pollution.

There are two major routes for the H_2SO_4 formation, either via hydrolysis of SO_3[4,5] or via direct oxidation of H_2SO_3.[6] The latter is believed to be a major precursor to sulfuric acid in the atmosphere. According to both experimental and theoretical studies, H_2SO_3 as well as HSO_3^- can be formed by the hydrolysis of SO_2.[7−9] The outcome of these reactions depends on environmental acidity. Other molecules such as NH_3 and atmospheric acids can contribute to the atmospheric hydrolysis of SO_2 by reducing the reaction energy barrier,[10,11] thereby facilitating the formation of H_2SO_3 and HSO_3^-. In addition, a wide variety of chemical species such as OH, OOH radicals, O_3, H_2O_2, and some organic compounds can play a role of oxidizing agents in the atmospheric conditions.[12]

Contrasting to their significances, the atomistic understanding of atmospheric H_2SO_4 formation mechanisms is relatively scarce. Recently, various theoretical oxidation mechanisms of H_2SO_3 and HSO_3^- by O_3 in the gas phase were proposed.[6] Based on the results, the authors[6] infer that the reaction $H_2SO_3 + O_3$ will play a minor role in the atmospheric H_2SO_4 formation due to the high energy barrier, whereas the $HSO_3^- + O_3$ reaction yielding HSO_4^- has a high probability due to the low energy barrier of 0.3 kcal/mol. Among other important oxidizing agents, H_2O_2 is one of the principal components of the oxidation process in the reaction path from SO_2 to H_2SO_4 in Earth's atmosphere.[12−14] Various possible oxidation mechanisms by H_2O_2 in laboratory experiments are described.[15] H_2O_2 can be split into $OH^\bullet$ radicals under light. If another H_2O_2 further reacts with the generated $OH^\bullet$, $HOO^\bullet$ can be formed. Both $HO^\bullet$ and $HOO^\bullet$ have a strong oxidizing ability. When H_2O_2 reacts with NaOCl, singlet oxygen $^1O_2$ can be formed which is a strong oxidizing agent as well.[16] Another mechanism proposed in previous theoretical studies is the formation of oxywater (H_2OO).[17−19] This isomer of H_2O_2 that is formed by a proton transfer from one O atom to the other is a short-lived reactive intermediate that is expected to play a significant role in different oxidative processes.

Here, ab initio calculations were performed to investigate detailed atomistic thermal mechanisms of H_2SO_3 oxidation by H_2O_2 into H_2SO_4 in our atmosphere without light. We considered two extreme conditions of pure gas phase as well as a heterogeneous moisturized environment. To study this, the

Received: June 7, 2019
Revised: September 4, 2019
Published: September 5, 2019

DOI: 10.1021/acs.jpca.9b05444
J. Phys. Chem. A 2019, 123, 8385−8390

effects of an additional water molecule as well as the polarized continuum model[20] (PCM) hydration model were studied.

2. COMPUTATIONAL METHODS

All of the geometry optimizations and the transition state searches were carried out using the General Atomic and Molecular Electronic Structure System (GAMESS) software package.[21] For the gas-phase calculations, a hybrid DFT functional with Becke exchange[22] and Lee−Yang−Parr correlation[23] (B3LYP)[24,25] was employed. The 6-31G* basis set[26,27] was used for all of the atoms: hydrogen, oxygen, and sulfur. All of the calculations were performed without assuming any point group symmetry.

3. RESULTS AND DISCUSSION

According to our study, it was found that there are many intermediates in the course of H_2SO_4 formation. If the initial formation energy of intermediates can be dissipated efficiently, stable intermediates are expected to be formed, which in turn increase subsequent reaction barriers. As a result, the overall reaction depends on the rate-limiting step with the largest reaction barrier E_D. This path can operate in high-temperature conditions. On the other hand, such a thermal equilibrium condition is not satisfied at low pressure. This is especially true in the upper troposphere of the Earth. In this condition, the initially formed intermediates cannot dissipate the excess of reaction enthalpy effectively, which can be utilized to overcome the subsequent reaction barriers. This corresponding barrier is referred to as nondissipative barrier or overall reaction barrier E_{ND} in this work.

Despite the H_2SO_3 + H_2O_2 model system being small, various oxidation pathways (mechanisms) were revealed due to a large number of possible reaction sites. Addition of one H_2O molecule to the above reactants further complicates reaction mechanisms. Both stepwise and concerted pathways were found for the reactions of H_2SO_3 + H_2O_2 without H_2O (shown in Figures 1 and 2, respectively). Even in the concerted pathways, three different mechanisms were revealed. In the presence of one H_2O molecule, both stepwise and concerted pathways were found (Figures 3 and 4, respectively). By considering the dissociation of H_2SO_3, again both stepwise and concerted pathways for the reaction HSO_3^- + H_2O_2 and one

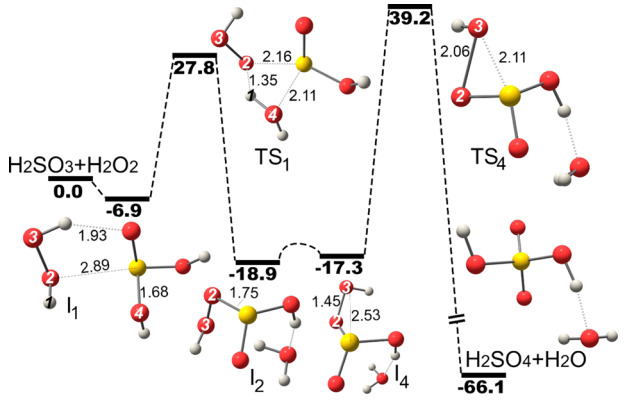

Figure 1. Energy profile and the optimized geometries for the stepwise pathway (***SP***) of the gas-phase reaction H_2SO_3 + H_2O_2. All distances are given in Å and energy values are in kcal/mol. Hydrogen, oxygen, and sulfur atoms are shown as white, red, and yellow balls, respectively.

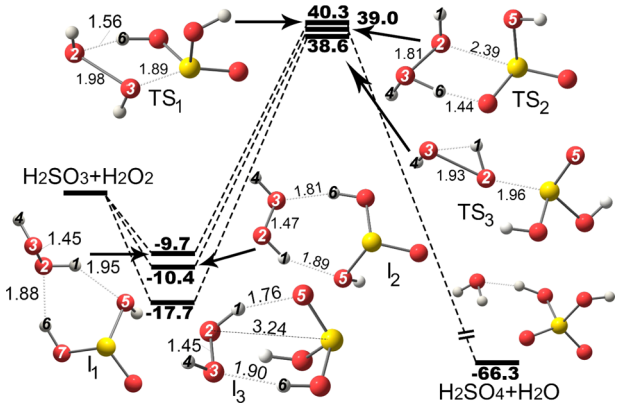

Figure 2. Energy profile and the optimized geometries for the concerted pathway (***CP***) of the gas-phase reaction H_2SO_3 + H_2O_2. The energy profiles and the optimized geometries are shown for all of the ***CP*** paths found. All distances are given in Å and energy values are in kcal/mol. Hydrogen, oxygen, and sulfur atoms are shown as white, red, and yellow balls, respectively.

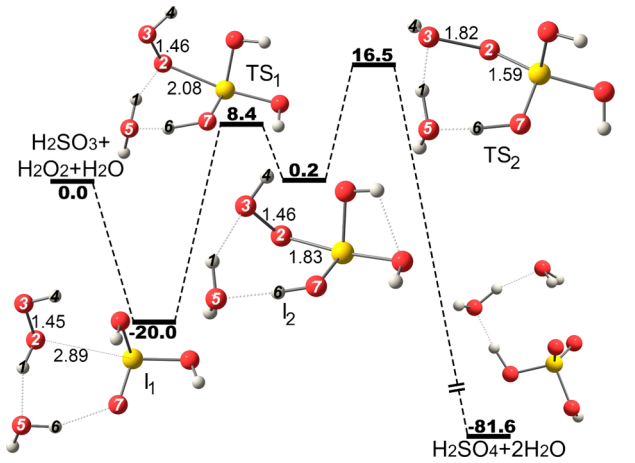

Figure 3. Energy profile and the optimized geometries for the stepwise pathway (SP_{H_2O}) of the reaction H_2SO_3 + H_2O_2 + H_2O. All distances are given in Å and energy values are in kcal/mol. Hydrogen, oxygen, and sulfur atoms are shown as white, red, and yellow balls, respectively.

concerted pathway for the reaction HSO_3^- + H_2O_2 + H_2O were revealed (Figures 5, 6, and 7, respectively). The following abbreviation is adopted throughout the article: **TS** stands for transition state and **I** for intermediate.

3.1. Reaction Mechanisms of H_2SO_3 + H_2O_2.

3.1.1. Stepwise Pathway with the Hydroperoxy Intermediate (SP). A stepwise pathway, which is denoted as ***SP*** (stepwise hydroperoxy path), is presented in Figure 1. For this pathway, the initial reactants are infinitely separated H_2SO_3 and H_2O_2 in the gas phase. The initial hydrogen-bonded complex ($\mathbf{I_1}$) is formed with the exothermicity of 6.9 kcal/mol. The proton transfer from O(2) to O(4) yields the first transition state $\mathbf{TS_1}$. During this process, the O(2)−H(1) and the S−O(4) bonds elongate from 0.98 to 1.35 Å and from 1.68 to 2.11 Å, respectively, while the S−O(2) distance shortens from 2.89 to 2.16 Å. This $\mathbf{TS_1}$ is characterized by the barrier of E_D = 34.7 kcal/mol with respect to $\mathbf{I_1}$ and E_{ND} = 27.8 kcal/mol with respect to the initial reactants. This $\mathbf{TS_1}$ connects $\mathbf{I_1}$ and another intermediate $\mathbf{I_2}$. The latter is composed of a peroximonosulfurous acid molecule HOSO(OOH) and H_2O

DOI: 10.1021/acs.jpca.9b05444
J. Phys. Chem. A 2019, 123, 8385−8390

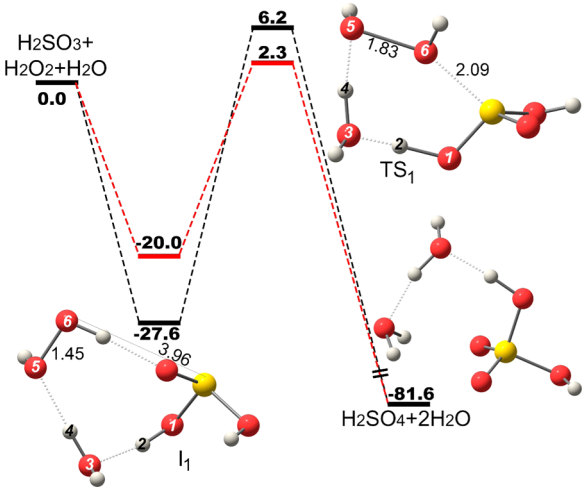

Figure 4. Energy profile and the optimized geometries for the concerted pathway (CP_{H_2O}) of the reaction H_2SO_3 + H_2O_2 + H_2O, both with (red) and without (black) PCM. All distances are given in Å and energy values are in kcal/mol. Hydrogen, oxygen, and sulfur atoms are shown as white, red, and yellow balls, respectively.

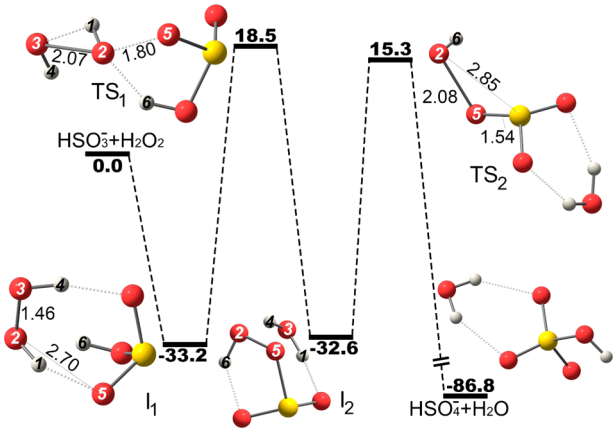

Figure 5. Energy profile and the optimized geometries for the stepwise pathway ($SP_{HSO_3^-}$) of the gas-phase reaction HSO_3^- + H_2O_2. All distances are given in Å and energy values are in kcal/mol. Hydrogen, oxygen, and sulfur atoms are shown as white, red, and yellow balls, respectively.

with an exothermicity of 18.9 kcal/mol with respect to the reactants. The formation of $\mathbf{I_2}$ is accompanied by further shortening the S−O(2) distance from 2.16 to 1.75 Å. It emphasized that this particular intermediate, in the form of an anion, was suggested experimentally.[28,29] A series of low-barrier conformational changes brings the $\mathbf{I_2}$ into $\mathbf{I_4}$ via the rotations of −O−O−H group along the S−O(2) bond (see Figure S1). The resulting $\mathbf{I_4}$ now has a hydroperoxy (−OOH) group that is in a favorable orientation for the attack of the S atom. Afterward, the attack occurs via $\mathbf{TS_4}$ in a nucleophilic addition (A_N)-like manner, i.e., the −OH group attacks the S atom by O(3). During this, the O(3)−O(2) bond elongates from 1.45 to 2.06 Å and the S−O(3) bond shortens from 2.53 to 2.11 Å. Finally, $\mathbf{TS_4}$ connects $\mathbf{I_4}$ and the final H_2SO_4 with the barrier E_D of 56.5 kcal/mol with respect to $\mathbf{I_4}$. This relatively high barrier appears due to the ring strain of S−O(2)−O(3). The nondissipative barrier E_{ND} also remains considerably high (39.2 kcal/mol). Although the overall

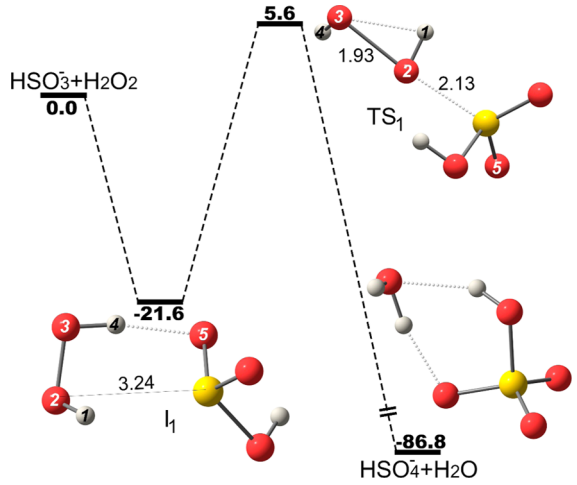

Figure 6. Energy profile and the optimized geometries for the concerted pathway ($CP_{HSO_3^-}$) of the gas-phase reaction HSO_3^- + H_2O_2. All distances are given in Å and energy values are in kcal/mol. Hydrogen, oxygen, and sulfur atoms are shown as white, red, and yellow balls, respectively.

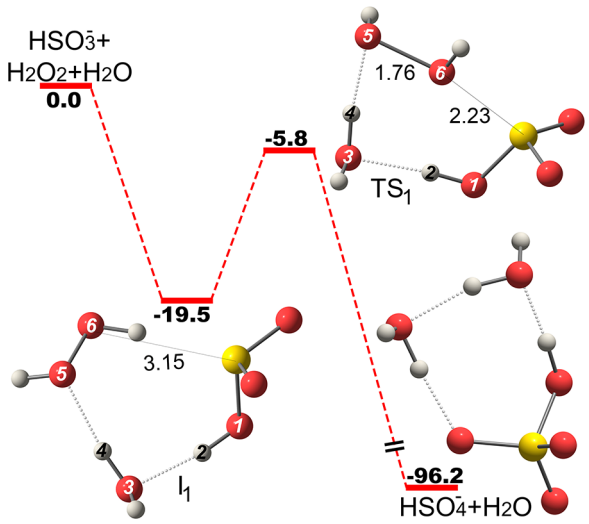

Figure 7. Energy profile and the optimized geometries for the concerted pathway ($CP_{HSO_3^-/H_2O}$) of the reaction HSO_3^- + H_2O_2 + H_2O with PCM. All distances are given in Å and energy values are in kcal/mol. Hydrogen, oxygen, and sulfur atoms are shown as white, red, and yellow balls, respectively.

reaction is highly exothermic (by 66.1 kcal/mol), a large reaction barrier makes the formation of H_2SO_4 through this particular path difficult. The largest E_D and the overall E_{ND} barriers are listed in Table 1 along with those of other reaction paths.

3.1.2. Three Concerted Paths of CP_1, CP_2, and CP_3. As compared to the stepwise path above, three different concerted mechanisms for the reaction between H_2SO_3 and H_2O_2 were found, and the results are shown in Figure 2. They are denoted as CP_1, CP_2, and CP_3, respectively. They all include the formation of double hydrogen-bonded complexes of $\mathbf{I_1}$, $\mathbf{I_2}$, and $\mathbf{I_3}$, respectively. The two hydrogen bonds H(1)−O(5) and H(6)−O(2) of $\mathbf{I_1}$ form a 6-membered ring intermediate with an exothermicity of 9.7 kcal/mol in comparison with the initial reactants. $\mathbf{TS_1}$ converts it into the final H_2SO_4 product with the significant E_D and E_{ND} barriers of 50.0 and 40.3 kcal/mol,

DOI: 10.1021/acs.jpca.9b05444
J. Phys. Chem. A 2019, 123, 8385−8390

Table 1. Reaction Energy Barriers E_D and E_{ND} (in kcal/mol) for Various Reaction Mechanisms of H_2SO_3 Oxidation by H_2O_2[a]

reaction path	E_D	E_{ND}
SP	56.5	39.2
CP_1	50.0	40.3
CP_2	49.4	39.0
CP_3	56.3	38.6
SP_{H_2O}	28.4	16.5
CP_{H_2O}	33.8 (22.3)	6.2 (2.3)
$SP_{HSO_3^-}$	51.7	18.5
$CP_{HSO_3^-}$	27.2	5.6
$CP_{HSO_3^-/H_2O}$	(25.3)	(−5.8)

[a]The values obtained from PCM calculations are given in parentheses.

respectively. During this process, the nucleophilic attack of O(3) on the S atom occurs simultaneously with the O(2)−O(3) bond elongation and the H(6) proton transfer to O(2). Here, the O(2)−H(6) distance decreases from 1.88 to 1.56 Å, whereas the O(2)−O(3) bond length increases from 1.45 to 1.98 Å. The reaction intermediate $\mathbf{I_2}$ of CP_2 path has a unique 7-membered ring and is slightly more stable than $\mathbf{I_1}$ by 0.7 kcal/mol, although a similar double hydrogen-bonded complex is formed. The concerted nucleophilic attack of O(2) on S and proton transfer of H(6) to O(3) in $\mathbf{TS_2}$ yields the final product. As compared to $\mathbf{TS_1}$, the nucleophilic attack is somewhat preceded by the proton transfer in $\mathbf{TS_2}$. The corresponding E_D and E_{ND} barriers are 49.4 and 39.0 kcal/mol, respectively, and are quite similar to those of CP_1. As compared to $\mathbf{I_1}$ and $\mathbf{I_2}$, the $\mathbf{I_3}$ intermediate of CP_3 is more stable by ∼7 kcal/mol. This is attributed to the hydrogen bonding between OH of H_2O_2 and O(5) that makes a double bond with S in H_2SO_3. In contrast, in both $\mathbf{I_1}$ and $\mathbf{I_2}$, OH of H_2O_2 is hydrogen bonded to OH of H_2SO_3. Its transition state $\mathbf{TS_3}$ is also different from the other two cases in terms of structure. Although the nucleophilic attack of O(2) on S is similar, a unique intramolecular hydrogen shift from O(2) to O(3) takes place. The E_D and E_{ND} barriers are 56.3 and 38.6 kcal/mol, respectively, which is comparable with the aforementioned two concerted paths.

In short, the reaction barriers of the three concerted mechanisms, i.e., CP_1, CP_2, and CP_3, are very close in energy with each other and far larger than the first barrier of the stepwise mechanism ***SP*** with the formation of a hydroperoxy intermediate. However, they are nearly as high as $\mathbf{TS_4}$ of Figure 1 making both stepwise and concerted paths not easily accessible.

3.2. Reaction Mechanisms of $H_2SO_3 + H_2O_2$ with H_2O. Two reaction pathways, i.e., a stepwise (SP_{H_2O}) and a concerted path (CP_{H_2O}) were found with an additional water molecule, and the results are shown in Figures 3 and 4 for SP_{H_2O} and CP_{H_2O}, respectively.

3.2.1. Stepwise Pathway with the Hydroperoxy Intermediate (SP_{H_2O}). For the first pathway (SP_{H_2O}) in Figure 3, the hydrogen-bonded interaction between the reactants yields a 6-membered ring intermediate ($\mathbf{I_1}$) with an energy gain of 20.0 kcal/mol, indicating that the extra water molecule further stabilizes the $H_2SO_3 + H_2O_2$ complex. The first transition state $\mathbf{TS_1}$ represents a nucleophilic attack of O(2) to S and a proton transfer relay of O(2) → O(5) → O(7), in which the extra water molecule serves as a bridge for the relay. This particular transfer chain significantly reduces both E_D and E_{ND} of $\mathbf{TS_1}$ by >6 kcal/mol and ∼20 kcal/mol, respectively, as compared to those without a water molecule (Section 3.1). The second intermediate ($\mathbf{I_2}$) of the formula $(HO)_3S(OOH)$ has a hydroperoxy group and is interesting because S is surrounded by three OH groups that is not common for this element. To the best of our knowledge, this compound has never been reported before, neither theoretically nor experimentally. This intermediate has a slight stabilization of 8.2 kcal/mol with respect to $\mathbf{TS_1}$. A reverse proton transfer of O(7) → O(5) → O(3) forms a second transition state $\mathbf{TS_2}$ with E_{ND} = 16.5 kcal/mol and finally yields two water molecules and H_2SO_4 with a large exothermicity of 81.6 kcal/mol. From the $\mathbf{I_2}$ intermediate, the reverse reaction to $\mathbf{TS_1}$ is preferred than the forward one to $\mathbf{TS_2}$ by 8.1 kcal/mol.

3.2.2. Concerted Path of CP_{H_2O}. In the case of the concerted path, as shown in Figure 4, the initial complex has three hydrogen bonds making a 9-membered ring structure with a significant exothermicity of 27.6 kcal/mol below the reactant energy level. The transition state $\mathbf{TS_1}$ represents a nucleophilic attack of O(6) on S and a proton transfer relay of O(1) → O(3) → O(5). The corresponding E_D and E_{ND} barriers are 33.8 and 6.2 kcal/mol, respectively, showing that the presence of a water molecule dramatically reduces the corresponding barrier heights by about 22.5 and 34.1 kcal/mol, respectively, as compared to the concerted pathway (Section 3.1). Additional PCM solvation calculations (represented as a red line) show even smaller E_{ND} barriers of 2.3 kcal/mol. Consequently, when the initial binding energy of $\mathbf{I_1}$ is not well dissipated, the small E_{ND} barrier of 6.2 (or 2.3 with PCM) kcal/mol can provide an efficient channel for H_2SO_4 formation.

3.3. Reaction Mechanisms of Deprotonated HSO_3^- with H_2O_2. Despite only 2% of H_2SO_3 (pK_{a1} = 1.81) being expected to dissociate into HSO_3^- and H^+ ions in the presence of moisture, the oxidation of HSO_3^- was studied as well. Both stepwise ($SP_{HSO_3^-}$) and concerted ($CP_{HSO_3^-}$) pathways were found and the results are shown in Figures 5 and 6, respectively.

3.3.1. Stepwise Path with the Hydroperoxy Intermediate ($SP_{HSO_3^-}$). The first reaction pathway is a counterpart of the stepwise mechanism ***SP*** (Section 3.1), due to the formation of deprotonated peroxymonosulfurous acid as an intermediate. The formation of the initial hydrogen-bonded complex ($\mathbf{I_1}$) is accompanied by the release of a significantly large amount of energy of 33.2 kcal/mol with respect to the separated reactants, showing a very strong interaction between the HSO_3^- anion and H_2O_2. By forming the O(2)−O(5) bond with simultaneous intramolecular proton transfer from O(2) to O(3), the transition state $\mathbf{TS_1}$ connects the initial complex with another intermediate ($\mathbf{I_2}$). The corresponding E_D and E_{ND} barriers are 51.7 and 18.5 kcal/mol, respectively. As compared to $\mathbf{TS_1}$ of Figure 1, E_{ND} is reduced by ∼9 kcal/mol. The intermediate ($\mathbf{I_2}$) is an anion of peroxymonosulfurous acid $(HOO)SO_2^-$, which was proposed and proven to exist previously in the experimental studies.[28,29] However, the mechanistic step of its rearrangement to HSO_4^- remained unclear. According to our study, this particular intermediate is converted to HSO_4^- by transferring the hydroxyl (−O(2)H(6)) to sulfur. The transition state $\mathbf{TS_2}$ represents this process with the internal barrier E_{ND} of 15.3 kcal/mol.

DOI: 10.1021/acs.jpca.9b05444
J. Phys. Chem. A 2019, 123, 8385−8390

3.3.2. Concerted Path of $CP_{HSO_3^-}$. Before studying the solvation effect, a simple bimolecular reaction of HSO_3^- with H_2O_2 was considered here. An intermediate $\mathbf{I_1}$ is characterized by the formation of a single hydrogen bond between H(4) of H_2O_2 and O(5) atom of HSO_3^- (see Figure 6). The energy gain in this intermediate formation step is as large as 21.6 kcal/mol in comparison with the reactants. Intramolecular proton transfer of H(1) from O(2) to O(3) takes place simultaneously with the elongation of the O(2)−O(3) bond and the nucleophilic attack of O(2) on the S atom, yielding the final HSO_4^-. $\mathbf{TS_1}$ describes this process with the E_D and E_{ND} barriers of 27.2 and 5.6 kcal/mol, respectively. The final product HSO_4^- + H_2O is formed with a high exothermicity of 86.8 kcal/mol. One can notice that the reaction path described is basically the same mechanism as that of $\mathbf{CP_3}$ (Section 3.1). However, in the case of HSO_3^-, the barrier is reduced significantly, i.e., by as much as 29 kcal/mol for E_D and by 33 kcal/mol for E_{ND}. Thus, if a nondissipative path is available, the reaction can easily occur.

3.3.3. Concerted Path of $CP_{HSO_3^-/H_2O}$. The reaction of HSO_3^- + H_2O_2 + H_2O is a counterpart of CP_{H_2O}. In the present case, the PCM model was applied to stabilize the negative charge on the O atom of HSO_3^- during the proton transfer from HSO_3^- to H_2O. The same reaction without the PCM model couldn't be located, since the proton transfers back to HSO_3^- due to the low stability of SO_3^{2-}. In this reaction, the initially formed complex $\mathbf{I_1}$ possesses similar features of CP_{H_2O} and is characterized by two hydrogen bonds of H(2)−O(3) and H(4)−O(5). The exothermicity during the $\mathbf{I_1}$ formation is 19.5 kcal/mol. After this, $\mathbf{TS_1}$ represents a nucleophilic attack of O(6) on S with a simultaneous proton transfer shift of O(1) → O(3) → O(5) and is characterized by E_{ND} = −5.8 kcal/mol. This barrier height is even lower than the already low E_{ND} of $CP_{HSO_3^-}$ (E_{ND} = 5.6 kcal/mol), indicating that the heterogeneous moisture environment in the atmosphere significantly accelerates the formation of HSO_4^-.

4. CONCLUSIONS

The thermal oxidation mechanisms of H_2SO_3 to H_2SO_4 by H_2O_2 in the gas phase were theoretically explored in the current study. The catalytic effect of one water molecule as well as the effect of the dissociation of H_2SO_3 on the overall oxidation reactions were also considered. To study the former effect, the reactants are H_2SO_3, H_2O_2, and H_2O, while those of the latter are deprotonated H_2SO_3 and H_2O_2. In all three cases, i.e., H_2SO_3 + H_2O_2, H_2SO_3 + H_2O_2 + H_2O, and HSO_3^- + H_2O_2, both stepwise and concerted mechanisms were found. The corresponding reaction barriers (see Table 1) were discussed with their energy dissipative and nondissipative aspects describing different scenarios of the reaction occurrence in the atmosphere.

One stepwise and three concerted pathways for the H_2SO_3 + H_2O_2 oxidation reaction were found. The stepwise mechanism proceeds via the formation of a peroxymonosulfurous acid (HOO)SO(OH) intermediate with a hydroperoxy group. According to our theoretical studies, all of these four paths have prohibitively large nondissipative reaction barriers (E_{ND}) of >38.6 kcal/mol, indicating that H_2O_2 alone would not convert H_2SO_3 to H_2SO_4. However, once a water molecule catalyzes the reaction, the E_{ND} barriers of both stepwise and concerted paths were dramatically reduced to 16.5 and 6.2 kcal/mol, respectively. With the PCM model, especially, the latter barrier even further reduces to 2.3 kcal/mol, providing a facile oxidation reaction forming H_2SO_4. For the stepwise mechanism, a previously unreported intermediate (HOO)S-$(OH)_3$ with S coordinated with three OH groups and a hydroperoxy group was found. The strong catalytic effect of a water molecule in the oxidation of H_2SO_3 was found to be due to its bridging role in proton transfer relay, which significantly reduces the intermolecular proton transfer barrier. In the case of deprotonated H_2SO_3 (HSO_3^- ion), a decrease of the reaction barriers was also observed. The corresponding E_{ND} barriers of the stepwise and concerted paths are reduced to 18.5 and 5.6 kcal/mol. With the PCM model, the concerted path further reduces to −5.8 kcal/mol, making the oxidation easily accessible. For the stepwise mechanism, the formation of a $(HOO)SO_2^-$ intermediate was observed, and the way it rearranges to HSO_4^- was revealed.

In short, the preferred concerted paths of CP_{H_2O} and $CP_{HSO_3^-}$ have the overall reaction barriers of 5−6 (2.3 to −5.8 with PCM) kcal/mol, showing the importance of catalytic effects of water and anionic HSO_3^- in the formation of H_2SO_4 in the atmosphere, even without sunlight.

■ ASSOCIATED CONTENT

Supporting Information

The Supporting Information is available free of charge on the ACS Publications website at DOI: 10.1021/acs.jpca.9b05444.

Cartesian coordinates of all of the optimized stationary points; stepwise pathway with the hydroperoxyl: intermediate rotations of −O−O−H group along S−O(2) bond (PDF)

■ AUTHOR INFORMATION

Corresponding Authors

*E-mail: papilio.podalirius@gmail.com. Tel: +82-53-950-5332 (Y.H.).

*E-mail: cheolho.choi@gmail.com. Tel: +82-53-950-5332 (C.H.C.).

ORCID

Kitae Kim: 0000-0003-0803-3547

Cheol Ho Choi: 0000-0002-8757-1396

Notes

The authors declare no competing financial interest.

■ ACKNOWLEDGMENTS

This work was supported by the Korea Polar Research Institute (KOPRI, PE19200).

■ REFERENCES

(1) Sipilä, M.; Berndt, T.; Petäjä, T.; Brus, D.; Vanhanen, J.; Stratmann, F.; Patokoski, J.; Mauldin, R. L.; Hyvärinen, A.-P.; Lihavainen, H.; et al. The Role of Sulfuric Acid in Atmospheric Nucleation. *Science* **2010**, *327*, 1243−1246.

(2) Weiss, R. E.; Waggoner, A. P.; Charlson, R. J.; Ahlquist, N. C. Sulfate Aerosol: Its Geographical Extent in the Midwestern and Southern United States. *Science* **1977**, *195*, 979−981.

(3) Yang, W.; Omaye, S. T. Air Pollutants, Oxidative Stress and Human Health. *Mutat. Res., Genet. Toxicol. Environ. Mutagen.* **2009**, *674*, 45−54.

(4) Reiner, T.; Arnold, F. Laboratory Investigations of Gaseous Sulfuric Acid Formation via SO_3+H_2O+M→H_2SO_4+M: Measure-

DOI: 10.1021/acs.jpca.9b05444
J. Phys. Chem. A 2019, 123, 8385−8390

ment of the Rate Constant and Product Identification. *J. Chem. Phys.* **1994**, *101*, 7399−7407.
(5) Hazra, M. K.; Sinha, A. Formic Acid Catalyzed Hydrolysis of SO_3 in the Gas Phase: A Barrierless Mechanism for Sulfuric Acid Production of Potential Atmospheric Importance. *J. Am. Chem. Soc.* **2011**, *133*, 17444−17453.
(6) Sheng, F.; Jingjing, L.; Yu, C.; Fu-Ming, T.; Xuemei, D.; Jingyao, L. Theoretical Study of the Oxidation Reactions of Sulfurous Acid/Sulfite with Ozone to Produce Sulfuric Acid/Sulfate with Atmospheric Implications. *RSC Adv.* **2018**, *8*, 7988−7996.
(7) Boniface, J.; Shi, Q.; Li, Y. Q.; Cheung, J. L.; Rattigan, O. V.; Davidovits, P.; Worsnop, D. R.; Jayne, J. T.; Kolb, C. E. Uptake of Gas-Phase SO_2, H_2S, and CO_2 by Aqueous Solutions. *J. Phys. Chem. A* **2000**, *104*, 7502−7510.
(8) Terraglio, F. P.; Manganelli, R. M. The Absorption of Atmospheric Sulfur Dioxide by Water Solutions. *J. Air Pollut. Control Assoc.* **1967**, *17*, 403−406.
(9) Chen, X.; Tao, C.; Zhong, L.; Gao, Y.; Yao, W.; Li, S. Theoretical Study on the Atmospheric Reaction of SO_2 with the HO_2 and $HO_2{\cdot}H_2O$ Complex Formation HSO_4 and H_2SO_3. *Chem. Phys. Lett.* **2014**, *608*, 272−276.
(10) Steudel, R. Sulfuric Acid from Sulfur Trioxide and Water - A Surprisingly Complex Reaction. *Angew. Chem., Int. Ed.* **1995**, *34*, 1313−1315.
(11) Liu, J.; Fang, S.; Liu, W.; Wang, M.; Tao, F. M.; Liu, J. Y. Mechanism of the Gaseous Hydrolysis Reaction of SO_2: Effects of NH_3 versus H_2O. *J. Phys. Chem. A* **2015**, *119*, 102−111.
(12) Calvert, J. G.; Lazrus, A.; Kok, G. L.; Heikes, B. G.; Walega, J. G.; Lind, J.; Cantrell, C. A. Chemical Mechanisms of Acid Generation in the Troposphere. *Nature* **1985**, *317*, 27−35.
(13) Penkett, S. A.; Jones, B. M. R.; Brice, K. A.; Eggleton, A. E. J. The Importance of Atmospheric Ozone and Hydrogen Peroxide in Oxidising Sulphur Dioxide in Cloud and Rainwater. *Atmos. Environ.* **2007**, *41*, 154−168.
(14) Pandis, S. N.; Seinfeld, J. H. Sensitivity Analysis of a Chemical Mechanism for Aqueous-Phase Atmospheric Chemistry. *J. Geophys. Res.* **1989**, *94*, 1105−1126.
(15) Lee, M.; Heikes, B. G.; O'Sullivan, D. W. Hydrogen Peroxide and Organic Hydroperoxide in the Troposphere: A Review. *Atmos. Environ.* **2000**, *34*, 3475−3494.
(16) Foote, C. S.; Wexlbr, S. Singlet Oxygen. A Probable Intermediate in Photosensitized Autoxidations. *J. Am. Chem. Soc.* **1964**, *86*, 3880−3881.
(17) Huang, H. H.; Xie, Y.; Schaefer, H. F. Can Oxywater Be Made? *J. Phys. Chem. A* **1996**, *100*, 6076−6080.
(18) Okajima, T. Ab Initio MO Study on the Solvent Effect for Hydrogen Shift from Hydrogen Peroxide (H_2O_2) to Water Oxide ($O{-}OH_2$). *J. Mol. Struct.: THEOCHEM* **2001**, *572*, 45−52.
(19) Jursic, B. S. Density Functional Theory and Ab Initio Study of Oxywater Isomerization into Hydrogen Peroxide. *J. Mol. Struct.: THEOCHEM* **1997**, *417*, 81−88.
(20) Gordon, M. S.; Schmidt, M. W. Advances in Electronic Structure Theory: GAMESS a Decade Later. In *Theory and Applications of Computational Chemistry*; Elsevier, 2005; pp 1167−1189.
(21) Becke, A. D. Density-Functional Exchange-Energy Approximation with Correct Asymptotic Behavior. *Phys. Rev. A* **1988**, *38*, 3098−3100.
(22) Lee, C.; Yang, W.; Parr, R. G. Development of the Colle-Salvetti Correlation-Energy Formula into a Functional of the Electron Density. *Phys. Rev. B* **1988**, *37*, 785−789.
(23) Becke, A. D. Density-Functional Thermochemistry. III. The Role of Exact Exchange. *J. Chem. Phys.* **1993**, *98*, 5648−5652.
(24) Stephens, P. J.; Devlin, F. J.; Chabalowski, C. F.; Frisch, M. J. Ab Initio Calculation of Vibrational Absorption and Circular Dichroism Spectra Using Density Functional Force Fields. *J. Phys. Chem. A* **1994**, *98*, 11623−11627.
(25) Francl, M. M.; Pietro, W. J.; Hehre, W. J.; Binkley, J. S.; Gordon, M. S.; DeFrees, D. J.; Pople, J. A. Self-consistent Molecular Orbital Methods. XXIII. A Polarization-type Basis Set for Second-row Elements. *J. Chem. Phys.* **1982**, *77*, 3654−3665.
(26) Hariharan, P. C.; Pople, J. A. The Influence of Polarization Functions on Molecular Orbital Hydrogenation Energies. *Theor. Chim. Acta* **1973**, *28*, 213−222.
(27) Cossi, M.; Barone, V.; Mennucci, B.; Tomasi, J. Ab Initio Study of Ionic Solutions by a Polarizable Continuum Dielectric Model. *Chem. Phys. Lett.* **1998**, *286*, 253−260.
(28) Purmal, A. P.; Sudachenko, E. A.; Travin, S. O. Kinetics of the Oxidation of Sulfite Ions by Hydrogen Peroxide. *Kinet. Catal.* **1997**, *38*, 470−473.
(29) Hung, H. M.; Hoffmann, M. R. Oxidation of Gas-Phase SO_2 on the Surfaces of Acidic Microdroplets: Implications for Sulfate and Sulfate Radical Anion Formation in the Atmospheric Liquid Phase. *Environ. Sci. Technol.* **2015**, *49*, 13768−13776.

DOI: 10.1021/acs.jpca.9b05444
J. Phys. Chem. A 2019, 123, 8385−8390